SIMSG ISSMGE

Paper No. 8.08

SECOND INTERNATIONAL CONFERENCE ON PERFORMANCE-BASED DESIGN IN EARTHQUAKE GEOTECHNICAL ENGINEERING

May 28-30, 2012 - TAORMINA (ITALY)

TOPOGRAPHIC EFFECTS EVALUATION FOR PERFORMANCE-BASED DESIGN

Ernesto AUSILIO [1], Paolo ZIMMARO[2]

ABSTRACT

The evaluation of ground motion intensity measures is an important component of Performance-Based Earthquake Engineering (PBEE). Pronounced variations in ground motion can occur between level sites and areas with irregular surface topography such as ridges, canyons, or slopes. This paper presents the results of numerical analyses of slopes under seismic waves.

The results show that these kinds of topographic irregularity may lead to intense amplification or de-amplification variability at neighboring points behind the crest of the slopes. Moreover, these analyses indicate that the amplification is highly frequency dependant and sensitive to the wave type and some measure of the topographic irregularity. There is no doubt that the presence of a slope plays a significant and important role in the spatial variation of the ground motion and therefore it is necessary to take this factor into account in the correct evaluation of the distribution of ground motion intensity measures (IMs).

Keywords: topographic effect, ground motion intensity measure, Boundary Element Method

INTRODUCTION

Performance-Based Earthquake Engineering (PBEE) can be considered as the coupling of expected levels of ground motion with desired levels of structural performance, with the objective of achieving greater control over earthquake-induced losses.

The development of this methodology includes four main analysis steps, in which the outcome of each step is mathematically characterized by one of four generalized variables: Intensity Measure (IM), Engineering Demand Parameter (EDP), Damage Measure (DM), and Decision Variable (DV).

The first step requires the evaluation of the distribution of ground motion intensity measures (IMs) at a site, given certain seismological variables. IMs may consist of traditional parameters such as spectral acceleration or duration, or newly defined parameters found to be useful for particular applications. An 'optimal' IM must possess efficiency, sufficiency, predictability, and scaling robustness (Bradley et al. 2009).

Given a particular set of IMs, the next step is to perform the evaluation of the distribution of engineering demand parameters (EDPs), which characterize the performance of a structure in engineering terms and can be calculated from response models (e.g. inter-storey drift for buildings; plastic hinge rotation for bridge columns and slope displacement for slopes).

The third step in the process is to perform a damage analysis, which relates the EDPs to Damage Measures, DMs. DMs include descriptions of the physical condition of a damaged element, with information on how the element would need to be repaired, and any life safety implications of the damage.

[1] Department of Difesa del Suolo, University of Calabria, e-mail: ausilio@dds.unical.it

[2] Department of Difesa del Suolo, University of Calabria, e-mail: paolo.zimmaro@unical.it.

The final step consists in calculating the probability of exceeding decision variables (DVs) within a given time period, given appropriate DMs. DVs describe human or collateral loss, post-earthquake repair time or other parameters that are meaningful for decision makers.

These four steps in the performance-based design methodology are linked through the theorem of total probability. Prediction of ground motions at a site is one of the most important issues of engineering seismology since this can provide a quick indication of the expected potential damage of future earthquakes Accordingly, high-quality ground motion characterization plays a vital role in PBEE.

The probabilistic evaluation of the distribution of ground motion intensity is associated with the following topics: source characterization, attenuation relations, near-fault ground motions, site effects, ground motion simulation and time history selection.

With particular reference to site effects, ground motion attenuation relationships provide estimates of intensity measures (IMs) that typically apply for broadly defined site conditions. Actual conditions at strong motion recording sites are significantly influenced by local ground conditions (geologic and local soil conditions), possible basin effects, and surface topography, and hence estimates from attenuation relationships are expressed in terms of averaged values across the range of possible site conditions. Analyses of site effects seek to improve the accuracy and reduce the dispersion of ground motion predictions using information about site conditions. Therefore, it is important to use models incorporating increasingly detailed site characterizations.

A series of studies has investigated the use of the simple and complex models for evaluating site effects. The simplest of these models are amplification factors defined on the basis of generalized site categories. Amplification factors are expressed as the ratio of a ground motion intensity measure for a specified site condition to the value of the parameter that would have been expected for a reference site condition. Amplification factors can be derived from observational data or numerical analyses. To account for this effect, attenuation functions for median spectral acceleration generally have a form in which a site factor appears (Steidl 2000; Stewart et al. 2001).

The nature of the role of this factor has been associated, in many previous studies, with the geological site effects. Most modern earthquake design codes present, for example, the variations of spectral shapes only in terms of $V_{s,30}$, which is the average shear-wave velocity in the top 30 m of soil at the site. The Eurocode 8 (EC8) uses the term ‘‘ground types’’ to categorize the site characteristics (Trifunac, 2012).

This methodology is applied generally for geological heterogeneity but intense variations in ground motion can occur between level sites and areas with irregular surface topography.

Certainly, in the recent past, there have been numerous cases of recorded motions and observed earthquake damage indicating topographic amplification as an important effect. Several reasonably well-documented case histories have been reported in the literature. The Tokachi-oki Earthquake (Japan, 1968), the San Fernando Earthquake (California, 1971), the Irpinia Earthquake (Italy, 1980), the Chile Earthquake (1985), the Eje-Cafetero Earthquake (Colombia, 1998) and recent earthquakes in Greece (Kozani-Grevena, 1995; Aigion, 1995; Athens, 1999) and Turkey (Bingol, 2003) are only some examples of catastrophic events, during which more severe and intensive structural damage has been reported on hilltops or close to steep slopes than those located at the base.

Furthermore, topographic site effects may play a significant role in the (re)activation of landslides and rockslides during earthquakes, which in many cases are one of the major causes of devastation. Well documented examples are the catastrophic Las Colinas landslide during El Salvador Earthquake (2001) and the Nevados Huascaran debris avalanche in Peru Earthquake (1970).

In recent years, numerous studies have investigated the influence of topographic effects on ground motion using both observational field data and theoretical and numerical studies. The majority of these studies focus on two-dimensional geometries in which the topographic irregularities are generally categorized as ridges, canyons and slopes.

The effects of slope topography on ground motion has been developed only in the last few years. The first studies were done by Boore (1972), Ohtsuki and Harumi (1983) and Ohtsuki et al. (1984).
Recently studies on this argument have been focused on parametric analysis, because the effects owing to slope topography on the ground motion are influenced by the type and the characteristics of incident wave, the incident angle, the frequency of excitation and some parameters that describe the geometry of the irregularity (Ferraro et al. 2009).
The studies of Ashford and Sitar (1997) and Ashford et al. (1997), have provided valuable insight into the effects of angle and height of slope, wave type (SH and SV) and wavelength, as well as the angle of wave incidence. The results of the analyses are presented solely at the crest and at some points, and they are obtained with the generalized consistent transmitting boundary method.
Bouckovalas and Papadimitriou (2005), through a numerical model based on the Finite Difference Method, conducted a parametrical analysis based on the hypothesis of uniform soil modeled with visco-elastic behavior, for a vertical SV wave propagation. The main parameters of the analysis are: slope inclination, normalized height, critical damping ratio and significant cycles of base excitation. The Authors have shown that the significant cycles and the soil damping have relatively minor effects. Moreover they have used a topography aggravation factors, defined as: $A_h = \frac{U_h}{U_{h,ff}}$ and $A_v = \frac{U_v}{U_{h,ff}}$, where U_h and U_v are peak horizontal and peak vertical accelerations at each point of the ground surface and $U_{h,ff}$ denotes the free-field value for the peak horizontal acceleration. For evaluating these factors and the distance to the free-field Bouckovalas and Papadimitriou proposed approximate relations.
Nguyen and Gatmiri (2007) conducted an extensive study on the influence of incident SV waves using the direct boundary element method.
Recently many studies have presented analysis based on real cases site-specific analysis (Athanasopoulos et al., 2001; Gazetas et al., 2002; Stewart and Sholtis, 2004).
These works underline without doubt that this kind of topographic irregularity may lead to intense amplification or de-amplification variability at neighboring points behind the crest of the slopes.
In this work are shown results about a numerical analysis performed with the Boundary Elements Method (BEM), on a slope. The method considers uniform soil modeling with linear-elastic behavior for incidence of harmonic P, SV and Rayleigh waves. The parametrical analysis is based on the variation of the inclination of the slope, and the normalized height, which, according to Bouckovalas and Papadimitriou (2005) are the main parameters that determine the influence of slopes on ground motion. This analysis is useful to understand that important amplifications are produced also with incident P and Rayleigh waves. Improving this kind of analysis with additional cases studies in the years ahead, it will be possible to develop a better empirical database on the importance of the Topographic Aggravation Factor.

ANALYSIS AND MODELLING

In the free-field condition a vertical propagation of SV waves produces only horizontal displacement. Similarly a vertical propagation of P waves produces only vertical displacement. The propagation of Rayleigh waves produces both horizontal and vertical displacements in the free-field condition. The free-field amplitudes for the above-mentioned waves are shown in Table 1. These values can be used for quantifying the effects of the presence of the irregularity. Noticeable differences are appreciable in the presence of topographic irregularity where the ground-motions are the product of superposing incoming SV (or P) waves, P and SV waves reflected at the ground surface and the Rayleigh waves locally generated by the interaction of diffracted waves with the free surface. The interference of all these waves results either in amplification or de-amplification.

The numerical application presented in this paper, to study the propagation of seismic waves in slopes is based on the resolution of the problem of the harmonic waves propagation by the Boundary Element Method (BEM). The method has certain inherent advantages and is highly suitable for dynamic problems involving semi-infinite domains. In particular, in this approach, the soil is modeled as a homogeneous isotropic elastic half-space with a Poisson's ratio ν=1/3. In this work, harmonic SV, P and Rayleigh waves are considered with a wavelength λ. The analyses are conducted with reference to incidence of the harmonic waves on a slope with variable angle of inclination (α). A schematic illustration of this model is reported in Figure 1.

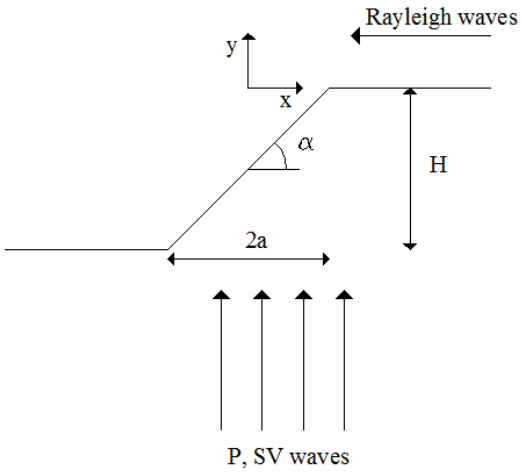

Figure 1. Schematic illustration of the model

where H is the height, 2a the width and α the angle of inclination of the slope.
The problem of the harmonic waves propagation in an linear elastic and isotropic medium is governed by the following equation:

$$\mu\nabla^2 u_t + (\Lambda + \mu)\nabla\nabla \cdot u_t + \rho\omega u_t = 0 \qquad (1)$$

where u_t is the displacement vector, Λ and μ are the elastic constants of the medium, ρ is the mass density and ω is the excitation frequency. In (1) the factor exp(iωt) is omitted, which describes the dependence of the displacement on time. For the linearity of the problem, it is possible to determine the displacement field u_t superimposing the contribute due to the incident, reflected and diffracted waves. The first two terms, corresponding to the free-field condition, are known, while the displacements associated with the diffracted waves are the unknowns. These displacements are calculated by the integration of (1) with the boundary conditions (Conte and Dente, 1992).
The solution may be obtained with the Boundary Elements Method, through the following relation:

$$C \cdot u = \int_S (u^* \cdot t - u \cdot t^*) dS \qquad (2)$$

where u and t are, respectively, the vectors of displacements and stresses on the surface due to the diffraction phenomena; u^* and t^* are the fundamental solutions to the problem, C is a 2x2 matrix whose terms depend, in general, on the position of the considered point. After the discretization of the surface, which should also be extended laterally to the slope, the equation (2) provides an algebraic system where the diffract displacements are unknown in the nodes.

After the calculation of the vectors u and t on the boundary, is possible to evaluate displacements and stresses in the internal point of the domain.

Table 1. Free-field displacement amplitude

Wave type	$U_{h,ff}$	$U_{v,ff}$
P	0	2
SV	2	0
Rayleigh	1	1.56

COMPARISON

In order to show the possible differences, it is instructive to compare the results calculated in this study to those obtained from other numerical methods publishing in the literature because there are no analytical solutions for step-like slope topography.

The first comparison is shown in Figure 2 where the distribution of the maximum horizontal (U_h) and vertical (U_v) surface displacements, normalized by the amplitude of the incident wave, are presented as function of the distance normalized by the half-width (a) of the slope. The input signal is a harmonic SV wave of unit amplitude with vertical incidence and $H/\lambda=0.25$. The results obtained in this study, for an angle slope $\alpha=60°$; are compared with those achieved by a method combining a particle model with a finite element analysis (Ohtsuki and Harimu, 1983). In Figure 3, another comparison, for vertically incident SV waves, is shown with the results obtained by using a direct boundary code named HYBRID (Nguyen and Gatmiri, 2007).

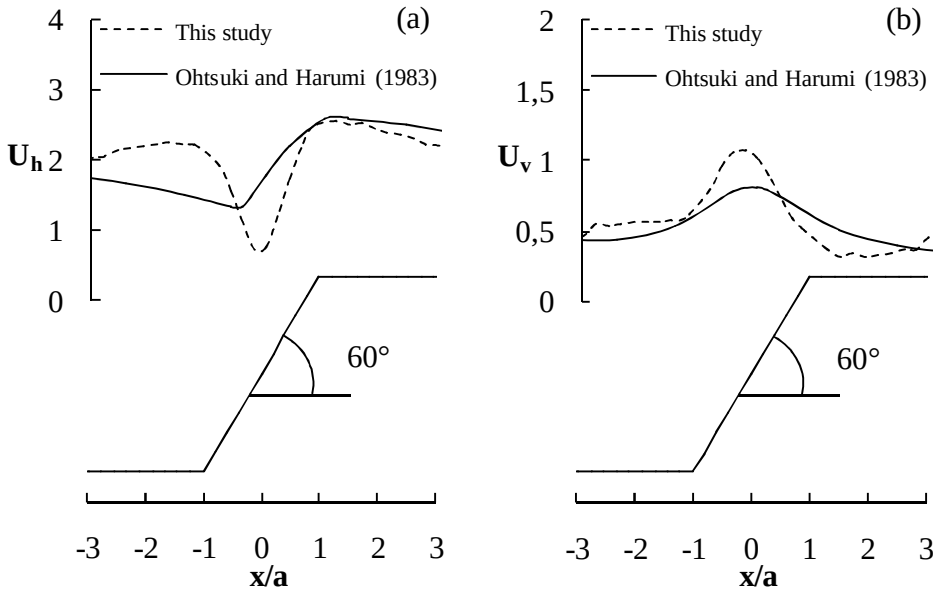

Figure 2. Distribution of the maximum horizontal (a) and vertical (b) surface displacements for vertically incident SV waves with H/l =0.25

The comparison in the case of incident Rayleigh waves is shown in Figure 4, where are presented the results obtained again by the method combining a particle model with a finite element analysis (Ohtsuki et al., 1984).

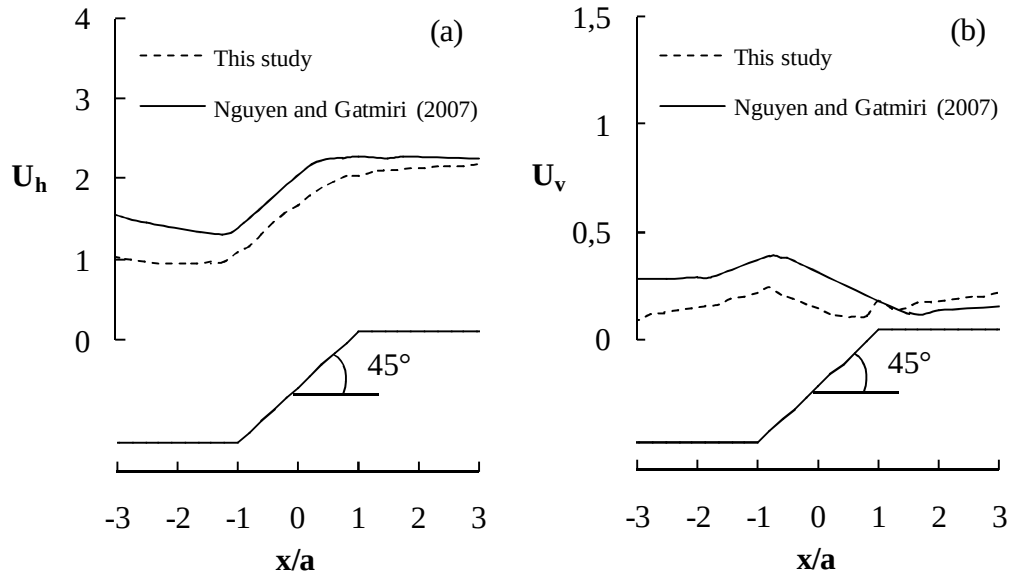

Figure 3. Distribution of the maximum horizontal (a) and vertical (b) surface displacements for vertically incident SV waves with H/l =0.125

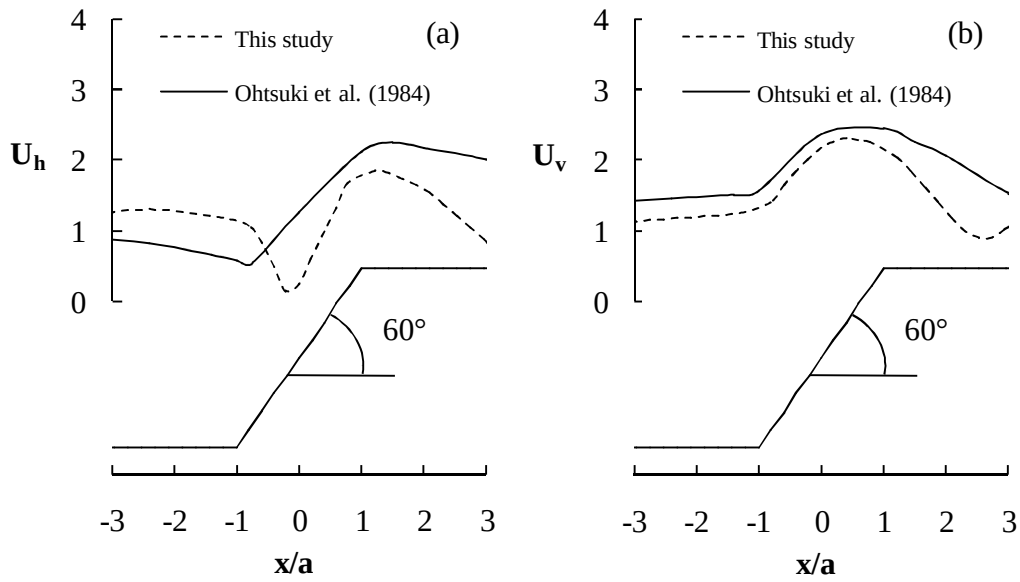

Figure 4. Distribution of the maximum horizontal (a) and vertical (b) surface displacements for incident Rayleigh waves with H/l =0.25

Finally, to explore the effects of excitation frequency on the ground motion the comparison between the results, in terms of horizontal and vertical amplification factor, of this study and those obtained by Ashford et al. (1997) with generalized consistent transmitting boundary method is shown in Figure 5.
It can be seen that the values of this study are in good agreement with other results.

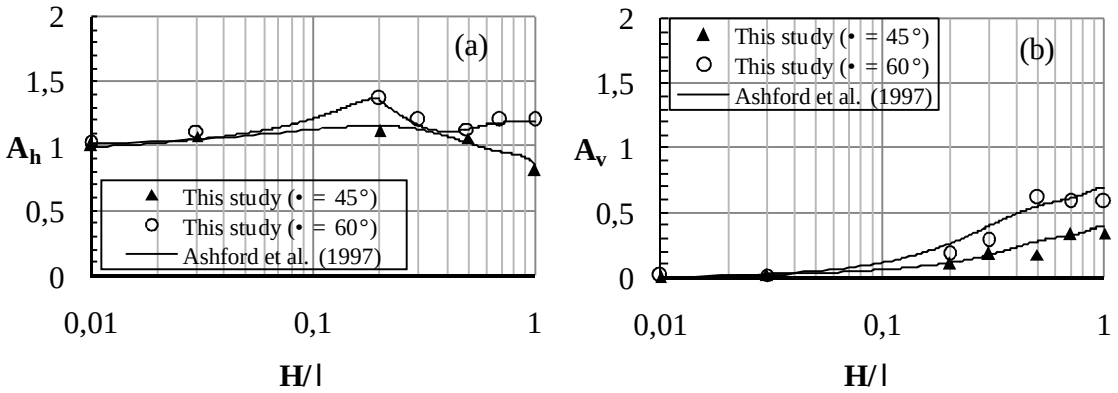

Figure 5. Horizontal (a) and vertical (b) amplification factor at the crest for vertically Incident SV waves

RESULTS

In this section, a series of calculations is carried out to illustrate the effect on ground motions of propagation of incident P, SV and Rayleigh waves. At first the influence of the harmonic vertically incident P waves is investigated. All results are given for a Poisson's ratio $\nu=1/3$. In Figure 6 and 7 the distribution of the maximum horizontal and vertical surface displacements for incident P waves with $H/\lambda=0.5$ are shown for angle slope $\alpha= 45°$ (Fig. 6a) and $\alpha=60°$ (Fig. 6b). It is important to remember that the free-field amplitudes for vertically incident P waves are: $U_{h,ff}=0.00$ and $U_{v,ff}=2.00$, as indicated in Table 1.

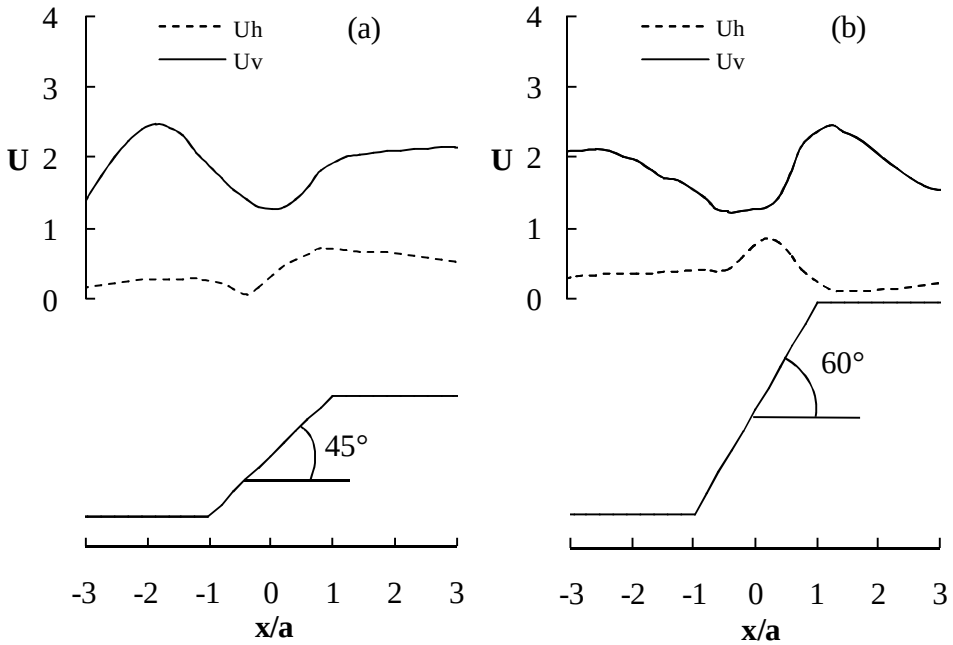

Figure 6. Distribution of the maximum horizontal and vertical surface displacements for incident P waves with H/l=0.5, a=45° (a) and a=60° (b)

It appears that the vertical surface displacement is amplified at the upper corner of the slope while the horizontal component of the surface displacement has the maximum value near the central part of the slope. Owing to the presence of the slopes that causes a complex wave scattering phenomenon, the horizontal surface displacement is non-zero. In order to investigate the effects of slope angle on ground motion, the distributions of horizontal and vertical surface displacement are plotted for different slope angle in Figure 7.
Some considerations can be made from the results shown in these figures. The surface motion is affected by the angle slope and the frequency of incident waves.

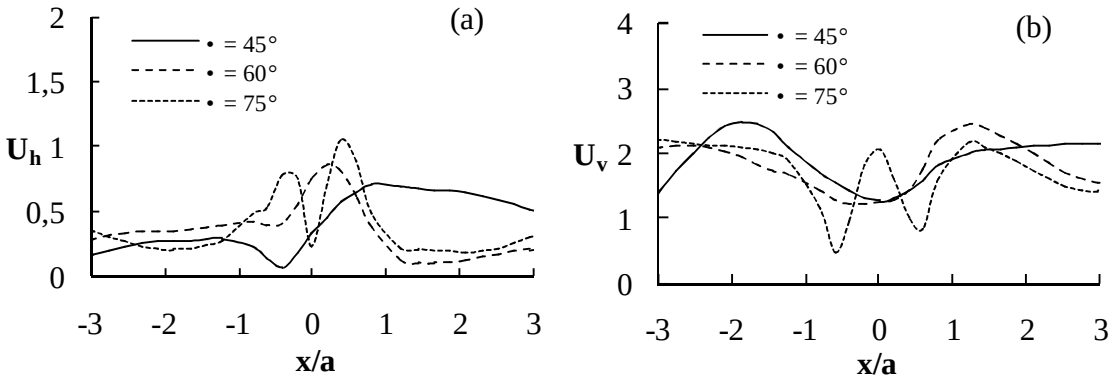

Figure 7. Distribution of the maximum horizontal (a) and vertical (b) surface displacements for incident P waves with H/l =0.5

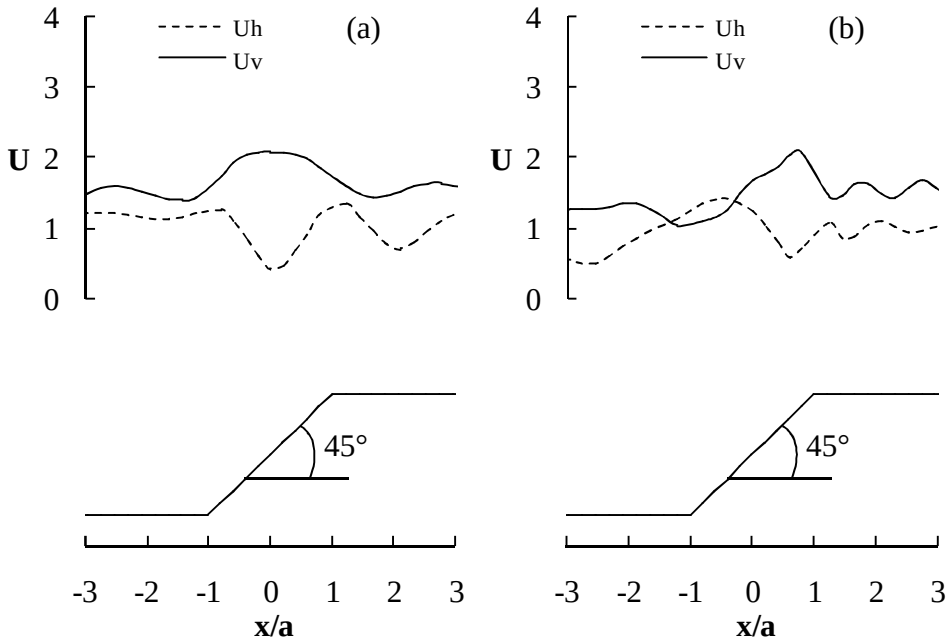

Figure 8. Distribution of the maximum horizontal and vertical surface displacements for incident Rayleigh waves with H/l =0.5 (a) and H/l =1 (b)

The distributions of horizontal and vertical surface displacements generated by a Rayleigh waves propagating from right to left are shown, for H/λ= 0.5, in Figure 8a and, for H/λ= 1.0, in Figure 8b. Figure 9 shows the same displacements for an angle slope α= 60° and for different values of normalized height.

To investigate the influence of slope angle on the horizontal and vertical displacements for incident Rayleigh waves, these displacements are plotted in Figure 10 for H/λ= 0.5 and α=45°-60°-75°.
It is important to note that the free-field amplitudes for incident Rayleigh waves are: $U_{h,ff}$=1.00 and $U_{v,ff}$=1.56, as presented in Table 1.

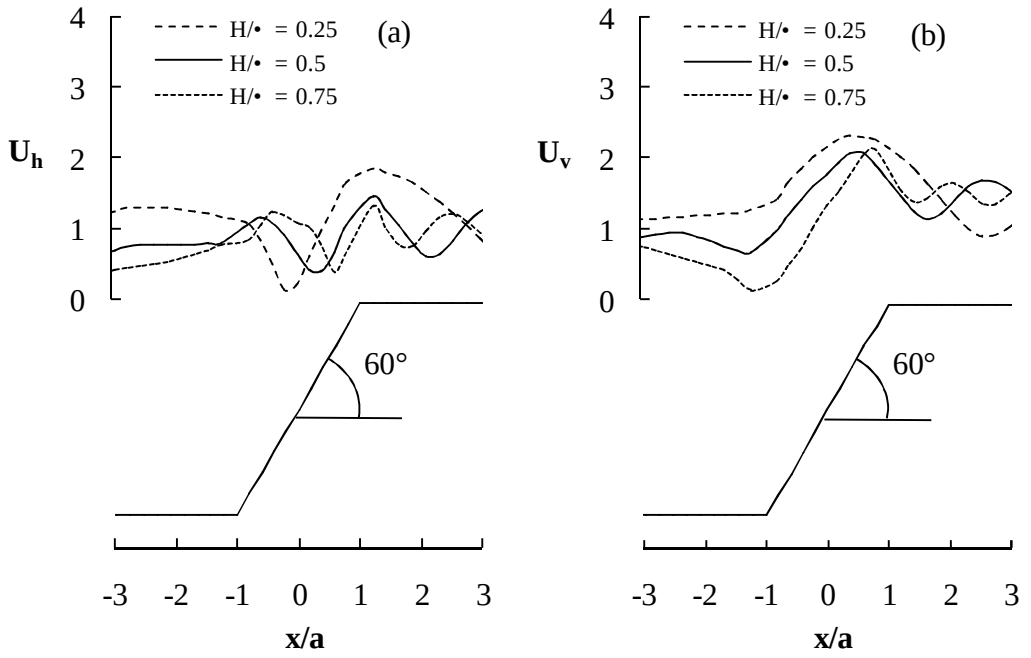

Figure 9. Distribution of the maximum horizontal (a) and vertical (b) surface displacements for incident Rayleigh waves with H/λ=0.25 -0.5 -0.75

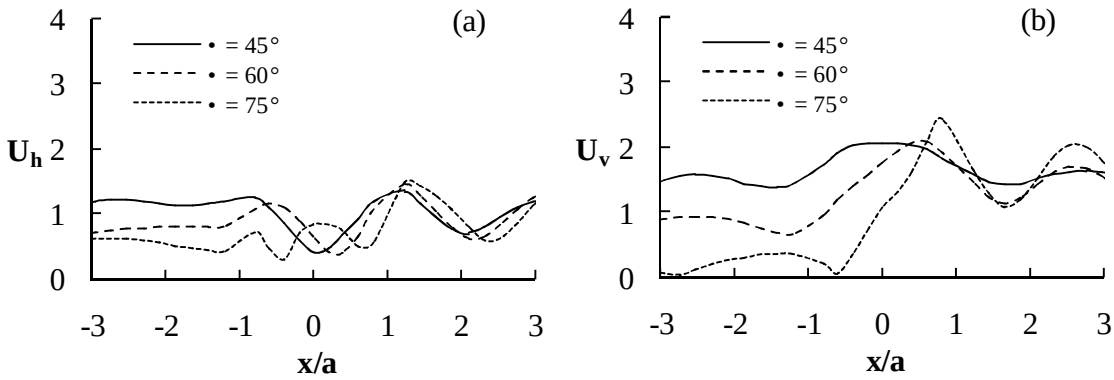

Figure 10. Distribution of the maximum horizontal (a) and vertical (b) displacements for incident Rayleigh waves with H/λ=0.5 and α=45°- 60°-75°

Finally, the distribution of the maximum horizontal and vertical displacements for vertically incident SV waves with H/λ= 0.5 and α=30°-45°-60° are shown in Figure 11.
As can be seen, the calculated values show amplification generally of about 1.3-1.5. Paolucci (2002) has demonstrated that this range of amplification may be responsible of an increase of macroseismic intensity (for example modified Mercalli intensity) up to one degree.

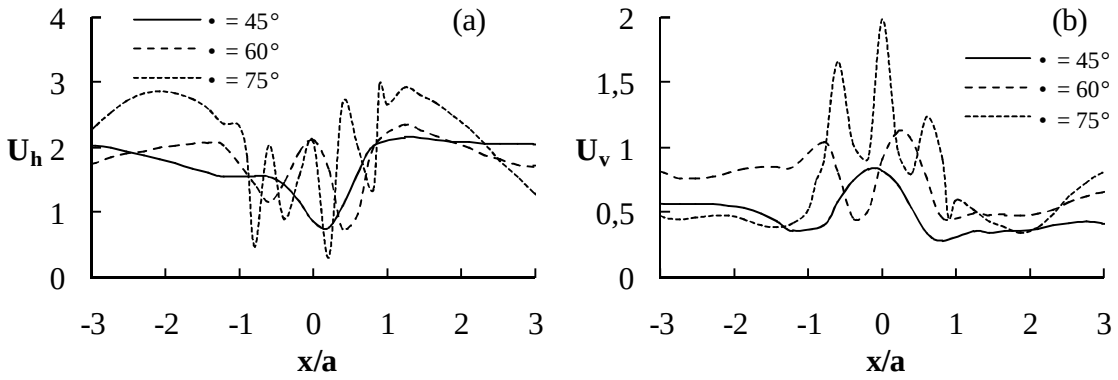

Figure 11. Distribution of the maximum horizontal (a) and vertical (b) displacements for incident SV waves with H/l =0.5 and a=30°-45°- 60°

SITE-SPECIFICAL ANALYSIS AND COMPARISON

In this section, the proposed method is applied to predict the results of three numerical case studies in which the equivalent linear finite element method has been used considering the actual seismic excitations. The first site examined is a slope of angle α=45° and height H=80 m at the northern part of Aigion during the 15 September 1995 Aigion earthquake in Greece. For this case, Bouckovalas et al. (1999) calculated a maximum amplification of the horizontal acceleration of the order of 1.40. Considering the approximate relations proposed by Bouckovalas and Papadimitriou (2005) the values of $A_{h,max}$=1.2-1.32 and $A_{v,max}$=0.12-0.31 are obtained. The results obtained in this study are: $A_{h,max}$=1.10-1.40 and $A_{v,max}$=0.05-0.18. These values were carried out considering vertically incident SV waves with a range of normalized height H/λ= 0.16-0.50 obtained taking into account the earthquake predominant period (0.4-0.5 s) and the gradually increasing shear wave velocity with depth (400-1000 m/s) (Tables 2 and 3).

The same analysis was performed for the area of Hotel "Dekelia" during the 7 September 1999 Athens earthquake in Greece. The topography is a slope with angle α=16° and height H=35m. The results of the site specific analysis are described by Athanasopoulos et al. (2001) while the comparison between the values obtained with various methods is summarized in Tables 2 and 3.

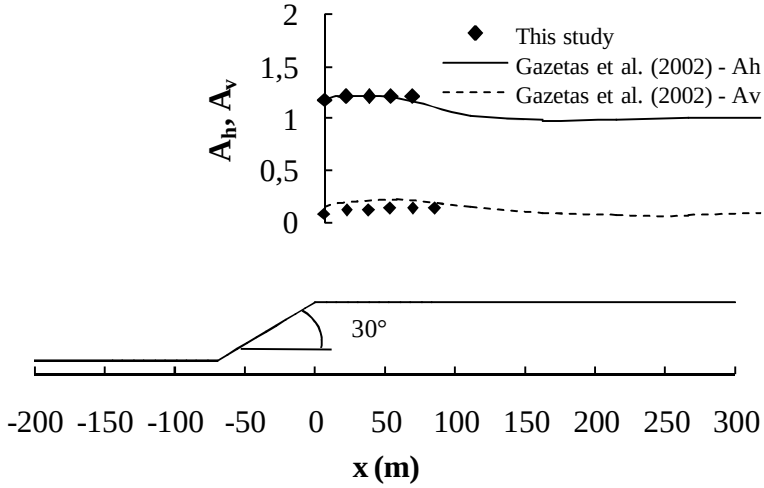

Figure 12. Amplification amplitude for horizontal and vertical direction compared with the results obtained by Gazetas et al. (2002)

Also the last numerical case study occurred during the 7 September 1999 Athens earthquake in Greece in the Adames area. In the site specific numerical analysis performed by Gazetas et al. (2002), the topography of the slope is characterized by an angle of about 30° and a height of 40 m. and the applied seismic excitations are recordings at other locations because there were no seismic recordings at the area of interest. Again the results and the comparisons are presented in Tables 2 and 3.
This last topography was analyzed by Gazetas et al. (2002) considering also a Ricker-type excitation with characteristic frequency of 3 Hz. The distribution along the ground surface of the normalized peak horizontal and vertical accelerations is shown in Figure 12 where also the results obtained in this study (SV wave vertical incidence) are reported for comparison.

Table 2. Results of site-specifical analysis (horizontal component)

Earthquake	Site	$A_{h,max}$ (site specific study)	$A_{h,max}$ (This study)	$A_{h,max}$* (Bouckovalas Papadimitriou 2005)
Aigion (1995)	Aigion city	1.40	1.10–1.40	1.20–1.32
Athens (1999)	Hotel "Dekelia"	0.75–1.35	1.06–1.24	1.16–1.25
Athens (1999)	Adames area	1.30–1.50	1.15–1.37	1.28–1.45

Table 3. Results of site-specifical analysis (vertical component)

Earthquake	Site	$A_{v,max}$ (site specific study)	$A_{v,max}$ (This study)	$A_{v,max}$* (Bouckovalas Papadimitriou 2005)
Aigion (1995)	Aigion city	–	0.05–0.18	0.12–0.31
Athens (1999)	Hotel "Dekelia"	–	0.05–0.12	0.11–0.27
Athens (1999)	Adames area	0.24-0.26	0.08-0.25	0.17–0.47

CONCLUSION

Some results are presented for the surface displacements generated in slopes by propagation of SV, P and Rayleigh waves. Computations are made using numerical procedure based on the boundary element method. On the basis of cases examined some features can be summarized as follows. The presence of the slopes alters the distribution of maximum surface displacements. In general, a zone of amplification takes place at the upper corner of slopes while a significant reduction of surface displacements occurs at the base of the slopes.
These variations of ground motion depend strongly on the frequency content of the excitation and slope geometry. For vertically incident P and SV waves the amplification is generally about 1.3-1.5. In addition, for incident SV waves, owing to mode conversion phenomena, a vertical component of motion is produced. The amplitude of this component is not insignificant and under certain conditions it may be as large as the horizontal. It has to be superimposed to that of the incoming excitation.
Similarly, for vertically incident P waves a horizontal component of motion is produced which is zero in free-field condition and it may become comparable to the vertical free-field motion. Large amplification values can be caused by Rayleigh waves and these effects must be considered in designing large structures.
The results obtained in this study, in accordance with many previous studies, show that the problem is complex, owing to the topographic irregularities which generate wave diffraction and scattering phenomena There is no doubt that the presence of a slope plays a significant and important role in the spatial variation of the ground motion and therefore it is necessary to take into account this factor in the correct evaluation of the distribution of ground motion intensity measures (IMs). A significant number of parameters affect model predictions of topographic effects. The lack of observation and experimental evidence for comparison and calibration of the findings of numerous numerical studies is a serious obstacle in generalizing their results.

This state of knowledge does not allow rigorous introduction of topographic effects within ground motion analysis procedures which are the first and vital step of performance-based design.
It is necessary to expand the records database introducing more detailed and accurate characterization of the topographic conditions and more records through installation of new accelerograph arrays deployed at carefully selected locations of the irregularity.
The interaction of seismic waves with slopes besides being important for local site seismic amplification and topographic effects affecting ground motion, is a major factor influencing landslide movements that involve slope stability.

REFERENCES

Athanasopoulos G. A., Pelekis P. C., Xenaki V. C. (2001). Topography effects in the Athens 1999 earthquake: the case of hotel Dekelia. Proceedings of fourth international conference on recent advances in geotechnical earthquake engineering and soil dynamics, San Diego, March (in CDROM).

Ashford A. S., Sitar. N. (1997). Analysis of topographic amplification of inclined shear waves in a steep coastal bluff. Bull Seismol Soc Am, Vol. 87, No. 3, pp. 692 – 700.

Ashford A. S., Sitar N., Lysmer, J. and Deng N. (1997). Topographic Effects on the Seismic Response of Steep Slopes. Bull Seismol Soc Am, Vol. 87, No. 3, pp. 701 – 709.

Bradley B. A., Dhakal R. P., MacRae G. A. and Cubrinovski M. (2009). Prediction of spatially distributed seismic demands in specific structures: Ground motion and structural response. Earthquake Engineering and Structural Dynamics

Bouckovalas G. D., Gazetas G., Papadimitriou A. G. (1999). Geotechnical aspects of the Aegion (Greece) earthquake. Proc.2° Intern. Confer. on Geotech. Earthquake Eng. Lisbon, June, Vol. 2, pp. 739 – 748.

Bouckovalas G. D. and Papadimitriou A. G. (2005). Numerical evaluation of slope topography effects on seismic ground motion. Soil Dynamics and Earthquake Engineering, Vol. 25, pp. 547 – 558.

Conte, E., Dente, G., (1992). Amplification effects of wave propagation in slopes. Proceedings of the French-Italian conference on slope stability in seismic areas, 1992, Bordighera, Italy, pp. 181–192.

Ferraro A., Grasso S. and Maugeri M.(2009). Site effects evaluation procedures for performance-based design. PBD in Earthquake Geotechnical Engineering – Tokyo pp. 377 – 383

Gazetas G., Kallou P. V., Psarropoulos P. N. (2002). Topography and soil effects in the MsZ5.9 Parnitha Athens earthquake: the case of Adames. Nat Hazards, Vol. 27, pp. 133 – 169.

Nguyen K. V. and Gatmiri B. (2007). Evaluation of seismic ground motion induced by topographic irregularity. Soil Dynamics and Earthquake Engineering, Vol. 27, pp. 183 – 188.

Ohtsuki A. and Harumi K. (1983). Effect of topography and subsurface inhomogeneities on seismic SV waves. Earthquake Engineering and Structural Dynamics, Vol. 11, pp. 441 – 462.

Ohtsuki A., Yamahara H and Harumi K. (1984). Effect of topography and subsurface inhomogeneity on seismic Rayleigh waves. Earthquake Engineering and Structural Dynamics, Vol. 12, pp. 37 – 58.

Paolucci R. (2002). Amplification of earthquake ground motion by steep topographic irregularities Earthquake Engineering and Structural Dynamics, Vol. 31, pp. 1831 – 1853.

Steidl J. H. (2000). Site response in southern California for probabilistic seismic hazard analysis. Bull Seismol Soc Am, Vol. 90, pp. 149 – 169.

Stewart J. P., Liu A. H., Choi Y., Baturay M.B. (2001). Amplification factors for spectral acceleration in active regions. Report. No. PEER-2001/10, PEER Center.

Stewart J. P., Chiou SJ., Bray J. D., Graves R.W., Somerville P.G. and Abrahamson N. A. (2002). Ground motion evaluation procedures for performance-based design. Soil Dyn. and Earth. Eng. pp. 765 – 772.

Trifunac M. D. (2012). Earthquake response spectra for performance based design—A critical review. Soil Dynamics and Earthquake Engineering, Vol. 37, pp. 73 – 83.